Journal of Fluorescence (2019) 29:1125–1131
https://doi.org/10.1007/s10895-019-02426-9

ORIGINAL ARTICLE

A Broad-Range Fluorescence Lifetime pH Sensing Material Based on a Single Organic Fluorophore

Christian Totland[1,2] · Peter J. Thomas[3] · Bodil Holst[4] · Naureen Akhtar[4] · Jostein Hovdenes[5] · Tore Skodvin[1]

Received: 30 May 2019 / Accepted: 29 July 2019 / Published online: 10 August 2019

Abstract

A general drawback for optical based pH sensors is that their response is typically limited to within 2–3 pH units centered around the pK_a of the indicator. Fluorescence lifetime (FL) is a particularly compelling basis for highly stable pH sensors since this is an intrinsic property of the indicator molecule. Here we demonstrate that it is possible to broaden the sensing range of FL based sensors significantly by placing the indicator in a support material where the indicator's chemical environment itself changes with pH. For acridine immobilized in amine-modified porous silica, a total FL change of 20 ns in the pH range 2–12 is achieved. A linear pH vs FL relationship is observed with three break points occurring at pH 4, 6 and 9 that are related to the pK_a values of the indicator and the silica material. This proves the concept that tuning the fluorophore's chemical environment can broaden the FL pH sensing range, where currently available fluorophores do not cover the full pH range.

Keywords Acridine · Fluorescence lifetime · Amine-modified silica · pH sensor · Solid-state NMR

Introduction

Optical based pH sensors are an alternative to the electrochemical sensor, where pH-induced changes in the indicator molecules result in various pH dependent spectroscopic responses. In this regard, fluorescence-based sensors have received much attention due to a potentially high degree of accuracy over a limited pH range of about 2–3 pH units about the pK_a of the indicator [1]. For several applications, such as in physiology or environmental monitoring, a narrow sensing range is sufficient and much effort has been directed towards development of optical pH sensors. However, in order to increase the applicability of the optical pH technology it is desirable to have a sensor that works over a broader pH range.

Several principles have been applied to broaden the sensing range beyond 2–3 pH units, particularly the use of multiple indicators with different pK_a values [2, 3]. For example, Stroble et al. were able to achieve a sensing range between pH 2–9 by applying four different fluorescent indicators [3]. Other approaches include the use of one indicator with multiple steps of acid dissociation, as well as photoinduced electron transfer where a single fluorophore is affected by various receptors (ionophores) with different pK_a values [4]. When considering fluorescent indicators, the pH sensing mechanism is protonation/deprotonation of functional groups in close vicinity to the aromatic rings, which leads to partial quenching of the fluorescence. Hence, a variation in the fluorescence *intensity* with pH about the indicator's pK_a is the most common effect for fluorescent indicators [5].

However, a particularly attractive optical property for pH sensing is fluorescence *lifetime* (FL). The motivation for using fluorescence lifetime rather than intensity to monitor pH is that FL is an intrinsic property of an indicator, which is not affected by e.g. leaching, light scattering effects, excitation

Electronic supplementary material The online version of this article (https://doi.org/10.1007/s10895-019-02426-9) contains supplementary material, which is available to authorized users.

✉ Christian Totland
christian.totland@ngi.no

[1] Department of Chemistry, University of Bergen, Allégaten 41, 5007 Bergen, Norway

[2] Present address: NGI – Norwegian Geotechnical Institute, Sognsveien 72, 0855 Oslo, Norway

[3] NORCE Norwegian Research Center AS, Fantoftvegen 38, 5072 Bergen, Norway

[4] Department of Physics and Technology, University of Bergen, Allégaten 55, 5007 Bergen, Norway

[5] Aanderaa – a Xylem brand, Sanddalsringen 5b, N-5225 Nesttun, Norway

source intensity variations or photobleaching. Therefore, FL can be a basis for more reliable sensors with long-term calibration stability, something that is not possible with electrochemical sensors. Although many indicators are available for intensity-based fluorescence pH measurements, very few of these show FL pH sensitivity. Consequently, the approaches mentioned above to broaden the pH sensing range are not currently possible for FL due to the very narrow selection of indicators. For physiological pH sensing, the fluorescein based indicator BCECF and fluorescent proteins are the most common. These exhibit a maximum lifetime response to pH of no more than 1–1.5 ns [5]. In fact, the only known organic indicator with a large pH induced FL response (20 ns) is acridine [6]. Hence, for a high-accuracy sensor based on an organic FL indicator, acridine is currently the only available candidate. Acridine has a pK_a of about 5.5, which limits its use as a pH sensor to the pH range of 4–7 (Fig. 1).

However, despite being stable in terms of e.g. leaching, variation in light scattering and photo bleaching, the FL will be affected by several variables related to the chemical environment of the indicator, including solvation dynamics, molecular rotation, polarity of the environments, Förster resonance energy transfer and charge transfer, among other things [5, 7]. Since the indicator needs to be immobilized in a solid matrix material for use in a sensor, the properties of this material is therefore important for the performance of the sensor.

For ruthenium(II) complexes with varying fluorescence intensity with pH, it has been shown that the pH sensing range can be broadened by approximately 2 pH units by immobilization in both hydrophobic and hydrophilic matrices [8, 9]. In this paper, we describe a system where pH-induced changes to the indicator's immobilizing matrix are used to obtain a significantly wider pH sensing range for the FL indicator acridine. The solid matrix material is amine-modified porous silica made by the sol-gel procedure using (3-Aminopropyl) triethoxysilane (APTES) and tetraethoxysilane (TEOS).

Experimental

Acridine (97%), (3-Aminopropyl) triethoxysilane (APTES, 98%) and tetraethoxysilane (TEOS, 98%) and were obtained

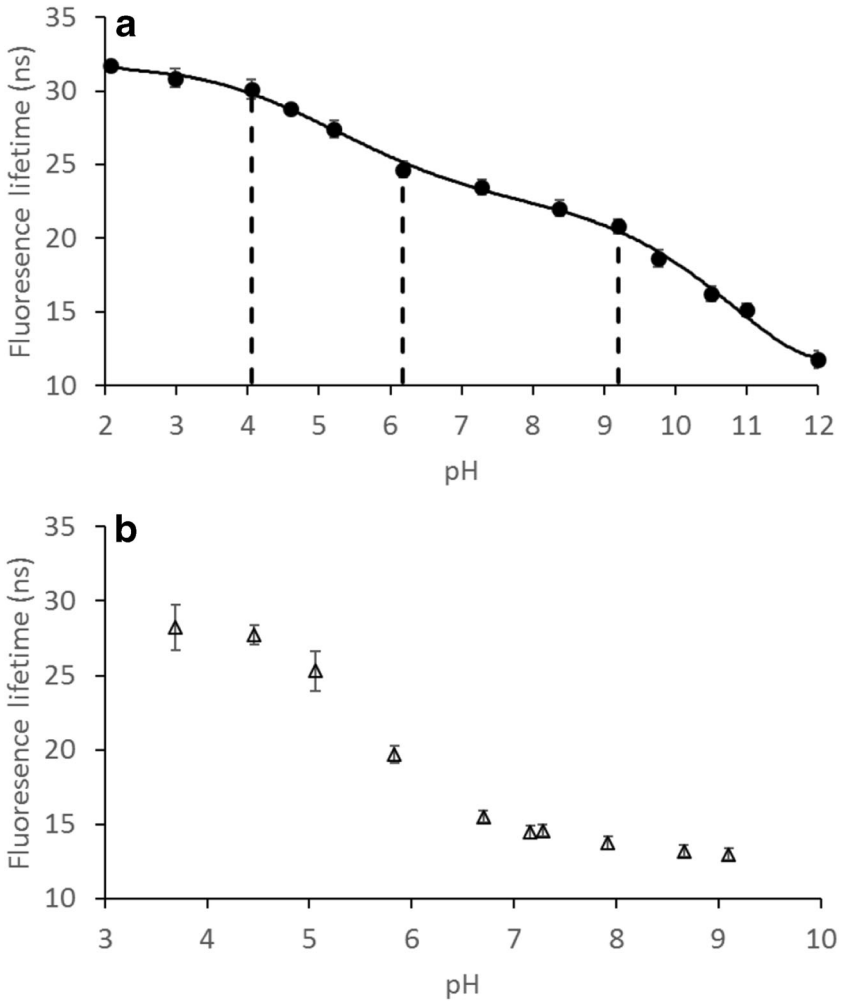

Fig. 1 **a** Fluorescence lifetime versus pH for acridine immobilized in the pores of amine-modified silica. The locations of three breakpoints are indicated by dashed lines. **b** Fluorescence lifetime versus pH for acridine dissolved in 100 mM buffer solutions

from Sigma Aldrich and used without further purification. The amine-modified silica was made by mixing 5 mL H_2O, 20 mL of 20 mM acridine in ethanol, 1 mL APTES and 0.93 mL TEOS for one hour. The material was then separated from the solution by centrifugation, followed by three rounds of washing with Milli-Q water. The samples that are used for fluorescence measurements have been mixed with Milli-Q water for an additional five days, after which leaching is negligible. Carmody Buffers were used [10], which were diluted to 100 mM due to the influence of electrolyte concentration on the pK_a of acridine.

Fluorescence Lifetime In obtaining the FL of the immobilized acridine, fluorescence excitation was stimulated using subnanosecond pulses from a PicoQuant PLS light emitting diode with emission centered at 380 nm. The resulting fluorescence was collected using a PicoQuant PMA 175 photomultiplier, fitted with a 45 nm spectral filter centered at 452 nm. The photomultiplier response was digitized using a TimeHarp 260 Nano. The fluorescence lifetime values reported were determined by fitting bi-exponential curves to the resulting fluorescence decay data using the FluoFit Pro software package. The lifetime values given are intensity weighted averages. The plotted uncertainties are derived from the confidence values for the best-fit parameters.

Soild-State NMR Spectroscopy The NMR experiments were obtained using a Bruker AVANCE III 500 MHz instrument. The instrument is equipped with a magic angle spinning (MAS) probe for 4 mm rotors. Experiments were carried out at a sample temperature of 298 K, with sample spinning rate of 10 kHz. For ^1H MAS NMR, water signal suppression was applied by pre-saturation pulses. ^{29}Si MAS NMR spectra were recorded using inverse-gated ^1H decoupling, 1000 transients and a relaxation delay of 120 s between each transient. Prior to packing the MAS rotors, the powdered samples were dispersed in D_2O, followed by sonication for 5 min to create a finer dispersion. The excess D_2O was removed by centrifugation at 18000 rpm, and the moist powder was packed into a rotor. D_2O was primarily added to increase the mobility of functionalized surface species of trapped acridine, in order to obtain a better resolution.

Leaching Leaching was tested by mixing a weighed amount (about 0.05 g) of powder / material in 5 mL water. Every hour for the five first hours 1 mL of the suspension was extracted, centrifuged, and the supernatant analyzed with UV spectroscopy. Then, samples were extracted and analyzed daily for five days. Exact concentrations of acridine were determined by comparison with a calibration curve for the UV absorption. The water needed to be replaced after the first hour as the amount of leached acridine approached the solubility limit in water of 0.25 mM.

Results and Discussion

In buffer solutions, acridine has a ~13 ns shift in FL over a relatively narrow pH range between pH 4 and 7 (Fig. 1b), which corresponds well with acridine's pK_a of 5.5. The total change in FL of about 20 ns is due to the FL difference between the protonated (31.6 ns) and neutral (6.6 ns) form of acridine [9]. However, when immobilized in amine-modified silica, the pH range is extended significantly due to pH-dependent changes occurring in the chemical environment of acridine (Fig. 1a). Between pH 4–6 and 9–11 there is a sharp drop in FL upon increase in pH of 2.5 ns per pH unit. From pH 6–9, and below pH 4, the FL changes 1 ns per pH unit. The highest accuracy for pH determination is therefore in the pH ranges 4–6 and 9–11. However, a change in FL of 1 ns per pH unit for the least sensitive pH ranges of immobilized acridine is still more or comparable to other known fluorophores within their most sensitive pH range, such as BCECF (0.6 ns/pH unit) used for fluorescence lifetime imaging (FLIM), and also fluorophores proposed for sensor candidates such as resorufin (1 ns/pH unit) [12]. Therefore, the material is a candidate for a FL pH sensor in the full range between pH 2–12.

As mentioned, numerous environmental factors may affect the FL of immobilized acridine, and the variation observed in the FL pH dependency between pH 2–12 indicates pH-induced migrations of the indicator between different chemical environments. These migrations are likely to have been induced by protonation/deprotonation of both the indicator and the silica material, which alters acridine's preferred binding sites. From a previous study using fluorescent nanoparticle adhesion assay, it was shown that amine-modified silica by APTES may have two pK_a values, one around 6.5 and one at about 9.9 [13]. However, reports on the pK_a of APTES varies somewhat depending on the method used and often include only one value [13–15]. These values are therefore used as approximates in the following analysis. The apparent pK_a of acridine varies depending on the chemical environment, and is for example sensitive to electrolyte concentrations. Acridine possesses both a ground-state pK_a (5.5) and an excited-state pK_a* value (10.6). In the heterogeneous microenvironment of porous silica, the thermodynamic equilibrium can be shifted and the apparent pK_a may differ from that measured in solution. For example, acridine immobilized in Nafion has an apparent pK_a of 9.1 and pK_a* of 9.39 in 100 mM electrolyte concentration at $\lambda = 450$ [11]. However, the complex microenvironment and non-sigmoidal plots obtained for acridine in amine-modified silica, complicate the determination of ground- and excited-state pK_a values. Nonetheless, the large difference in lifetime between neutral and protonated acridine species is maintained when immobilized in the silica, as seen from Fig. 1b. The FL of acridine is particularly sensitive to the polarity of its environment, where lower polarity reduces the FL, as well as both emission intensity and wavelength [16].

Figure 2 shows three possible adsorption sites for acridine in the silica material; a) hydrophobic interactions with the propyl chain, b) electrostatically bonded to surface $–O^-$ groups, and c)&d) H-bonded to surface amine groups. The latter can only take place when acridine is neutral (non-protonated) and hydrogen bonds between its unpaired electrons and surface primary amine hydrogen atoms can occur. When both amines are protonated, on the other hand, repulsion occurs.

Similarly, neutral acridine can form H-bonds to surface hydroxyls. In this system, deprotonation of the silanols will likely occur to a larger extent at lower pH values than what is the case for amorphous silica in general, due to the amine functionalization. Isolated silanols have a lower pK_a at around 4.5, whereas vicinal silanols H-bonded to each other have a pK_a at around 8.5 [17, 18]. ^{29}Si magic angle spinning (MAS) NMR shows that the ratio between the various Si species Q2/Q3/Q4/Si-CH_2- is 3.5/31.5/45.5/19.5 (see Supporting Information). This e.g. implies a Si-CH_2-/Si-OH ratio of 1/3, and a Q2/Q3 ratio of 1/10, indicating that a larger proportion of silanols will be isolated and negatively charged at neutral pH, although pK_a 8.5 silanols will of course occur to some extent.

However, the cationic protonated acridine can bind electrostatically to the deprotonated anionic silanols, which is the strongest possible binding situation for acridine. The attraction between the aromatic rings and the propyl chain will be driven largely by entropy, as is the case with aggregation of nonpolar groups in general [19], and is the weakest form of attraction. Another environmental factor is the surface-bound water. Ionization of the surface hydroxyl and amine groups can alter the structural organization of the water, which in turn can affect the FL of acridine by both altered molecular dynamics and solvent polarity [20]. Hence, the chemical environment of acridine immobilized in this material is complex and will change with pH.

Based on the adsorption sites where acridine is likely to reside at different pH values (Fig. 2), it is possible to reason the wide pH sensing range of this material. As the pH increases above pH 2, the silica surface will gradually become anionic due to deprotonation of isolates silanols [21]. At such low pH values, acridine remains protonated and electrostatic attraction between the cationic acridine and anionic surface sites occurs. This can move acridine from a less polar environment (propyl chains) to a more polar one. Electrostatic attraction is strong compared to the other possible types of

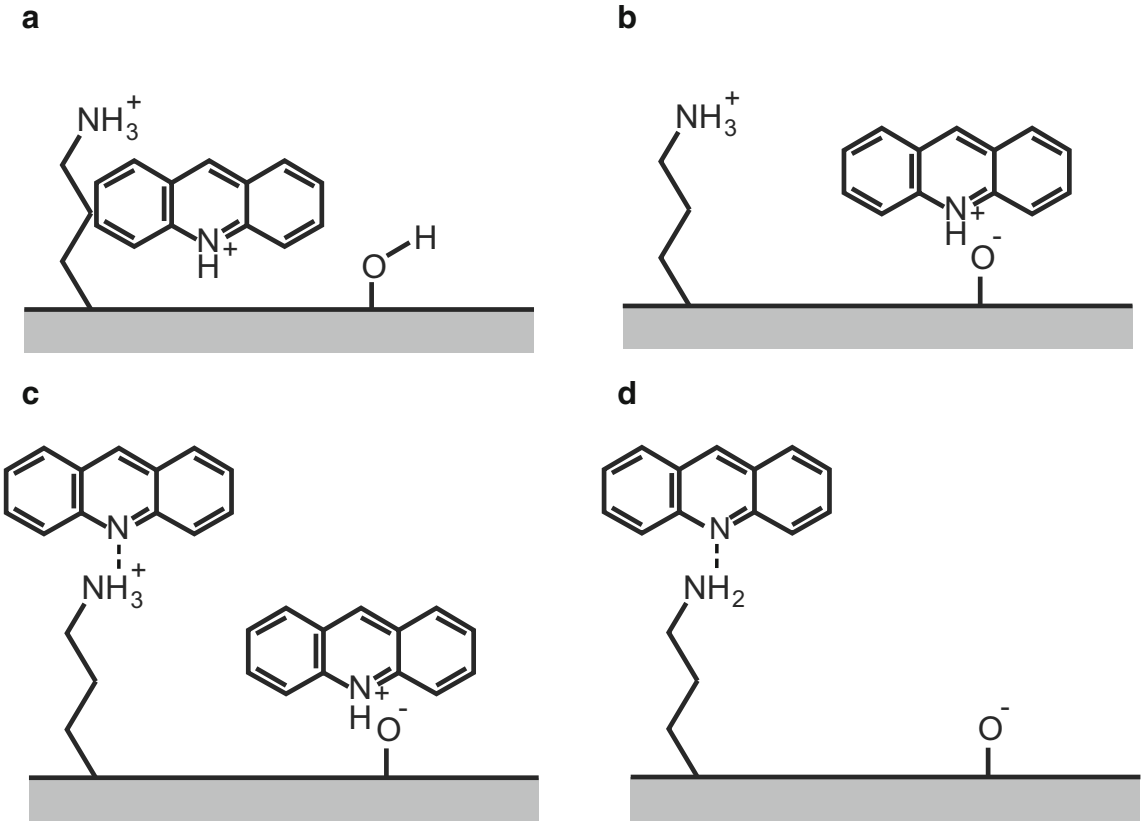

Fig. 2 Schematic representation of possible adsorption sites for acridine in the amine-modified silica material at different pH values: **a** Hydrophobic interaction with the surface propyl chain. This is a probable adsorption site at low pH where most surface sites and acridine are protonated. **b** Electrostatic interaction between acridine and deprotonated surface silanols occurs at acidic pH values, i.e. when acridine is protonated. **c** Neutral acridine can form H-bonds to surface-NH_3^+ groups. d) At pH > 6.5 surface amines will start to deprotonate. Most acridine is deprotonated and electrostatic interaction with surface $–O^-$ groups occurs to a lesser extent

acridine surface binding, and it is probable that a certain amount of acridine will reside near the surface hydroxyls as long as acridine itself is protonated. The slight 2 ns decrease in FL on going from pH 2–4 is therefore likely related to the deprotonation of the surface hydroxyls and consequent binding of protonated acridine to these.

At pH values above 4 there is a sharper decrease in FL with increasing pH, indicating the onset of acridine deprotonation, which is the principal source of increase in FL. This reduces both electrostatic attraction to anionic surface sites, and repulsion to the cationic surface $–NH_3^+$ groups. Neutral acridine is further capable of H-bonding. A new possible destination for the deprotonated acridine is therefore the surface amine groups, as well as silanols that remain protonated at this pH. The next breakpoint in the curve (Fig. 1a) occurs at pH 6, which approximately corresponds to the first pK_a of the surface amines. According to Fig. 1, much acridine remains protonated at pH 6, and deprotonation of the surface $–NH_3^+$ groups will therefore reduce repulsion between protonated acridine and the surface amines further.

The final breakpoint in the curve occurs around pH 9. This may correspond to both the pK_a of H-bonded/vicinal silanols (around 8.5) or the second pK_a of amine modified silica (around 9.9). Furthermore, the electrostatic interaction between protonated acridine and anionic $–O^-$ groups may delay deprotonation of some acridine, and it is possible that this breakpoint is related to the higher pK_a obtained by such acridine. Electrostatic binding of protonated acridine to anionic sites is e.g. also proposed as an explanation for the higher pK_a of 9 for acridine in Nafion [11]. No explanation is given in literature for the occurrence of the second pK_a for silica modified with APTES [13], and should the final break point observed in Fig. 1a be related to this, the explanation remains elusive.

^{1}H MAS NMR (Fig. 3) confirms that acridine is present at several binding sites simultaneously. Figure 3 compares the spectra of acridine in D_2O wetted amine-modified silica and acridine dissolved in D_2O. The chemical shifts of ^{1}H resonances of acridine in the amine-modified silica corresponds to those of acridine dissolved in water. However, at least two additional peaks appear (marked with asterisk in the spectrum). The larger additional peak is shifted 0.27 ppm downfield from resonance ‘b,e’.

In an aqueous solution with presence of both protonated and non-protonated acridine, the dynamics (protonation/deprotonation) is very fast on an NMR time scale, which

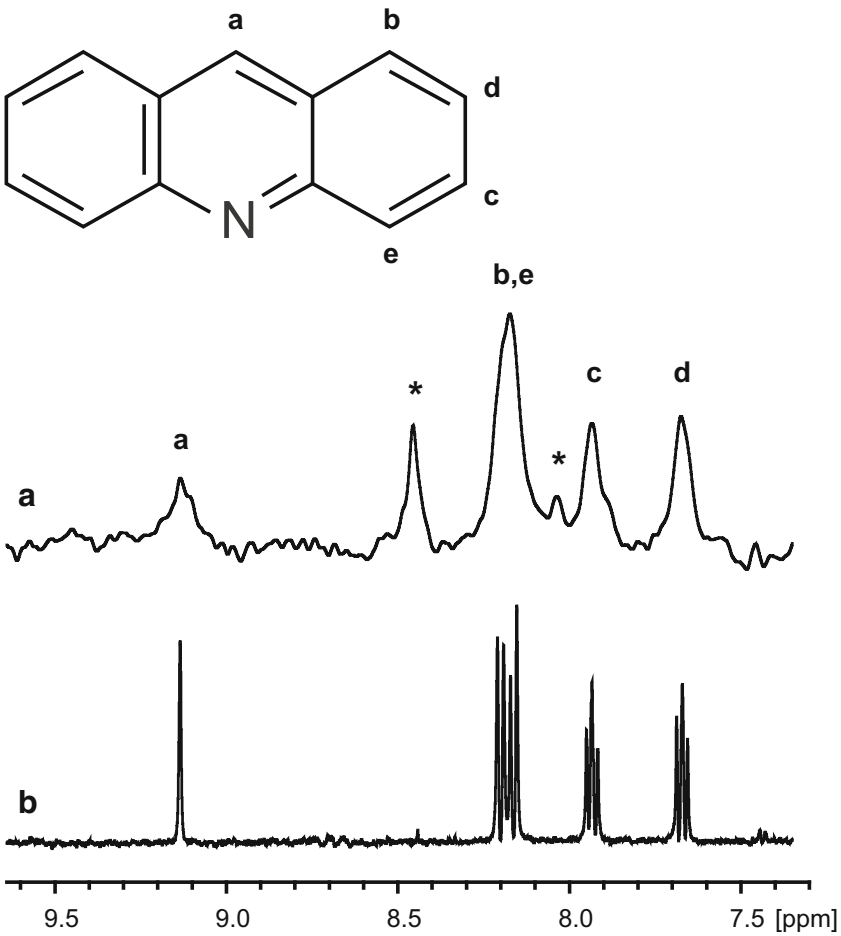

Fig. 3 **a** ^{1}H MAS NMR spectrum (10 kHz MAS) of acridine in amine-modified wetted (D_2O) silica. **b** ^{1}H NMR spectrum of acridine dissolved in D_2O

prevents observation of two peaks, but rather one peak with a weighted average chemical shift. In order for two peaks to be observed, a more stable configuration is required. Higher ppm values mean higher electron density about the nucleus, and can be rationalized by stronger solvent interactions. Shifted bond polarization caused by either H-bonding or electrostatic interactions can potentially also cause changes in chemical shift – proton e is the proton closest to the nitrogen involved in such bonding, only separated by two bonds, and this is thus another plausible explanation. Electrostatic bonding of acridinium to anionic sites may prevent deprotonation [11], which in turn can slow the dynamics sufficiently for two peaks to be observed. The NMR data gives no explanation to the specific nature of the two observed adsorption sites, although it is interesting to note that the additional acridine peaks are not observed when the material is wetted with an acidic buffer (Supporting Information), indicating that the additional peaks are related to an adsorption site that is not present at lower pH.

Leaching of acridine was measured in distilled water (Supporting Information). Following the three-step washing procedure (see Methods), a small amount of powder was left tumbling with water. The dispersion was centrifuged and the supernatant analyzed for leached acridine. Within the first hour, 8% of the original amount of acridine (after washing) had leached. After six hours, 10% of the acridine had leached, after which no measureable amount of acridine leaches the following five days. Hence, the leaching is manageable in terms of use in a sensor.

In conclusion, we have shown that the high sensitivity of fluorescence lifetime to the chemical environment of a single organic fluorophore, in this case acridine, can be exploited to obtain a wide-range pH sensor. Similar to other methods for widening the pH sensing range of optical pH sensors, such as the use of multiple indicators or ionophores, or indicators with multiple steps of acid dissociation, our method relies on the presence of multiple components with different pK_a values. However, here the additional pK_a components are associated with the immobilizing matrix itself.

It should be noted that for a re-usable sensor based on this principle, covering pH values lower than 4 and/or greater than 9, a polymer support should be applied due to degeneration of silica at high/low pH. However, this study proves the concept of applying pH mediated environmental changes to adjust the sensing range of an organic fluorophore in an FL based pH sensor.

Due to the high total change in fluorescence lifetime of acridine between high and low pH, an acridine-based material can be able to resolve relatively small pH changes over a broad pH range. One limitation with the use of acridine is its sensitivity to chloride, which quenches the fluorescence of protonated acridine at chloride concentrations above about 20 mM [11, 22]. However, semipermeable membranes such as Nafion are able to protect the indicator from chloride [11]. Another fluorophore known for its long fluorescence lifetime is pyrene, and pyrene derived indicators are other potential candidates for fluorescence lifetime sensors. Diethylaminomethyl pyrene has e.g. been shown to have potential as a sensitive fluorescence lifetime pH sensor in the past [23], and could be an alternative for acridine. However, a drawback with pyrene derived indicators is their high sensitivity to oxygen [7].

Acknowledgements The present study was supported by the Research Council of Norway (grant number 269090), and by Aanderaa – a Xylem brand.

References

1. Wencel D, Abel T, McDonagh C (2014) Optical chemical pH sensors. Anal Chem 86:15–29
2. Lin J, Liu D (2000) An optical pH sensor with a linear response over a broad range. Anal Chim Acta 408:49–55
3. Strobl M, Rappitsch T, Borisov SM, Mayr T, Klimant I (2015) NIR-emitting aza-BODIPY dyes - new building blocks for broad-range optical pH sensors. Analyst 240:7150–7153
4. Qi J, Liu D, Liu X, Guan S, Shi F, Chang H, He H, Yang G (2015) Fluorescent pH sensors for broad-range pH measurement based on a single fluorophore. Anal Chem 87:5897–5904
5. Berezin MY, Achilefu S (2010) Fluorescence lifetime measurements and biological imaging. Chem Rev 110:2641–2684
6. Ryder AG, Power S, Glynn TJ, Morrison JJ (2001) Time-domain measurement of fluorescence lifetime variation with pH. Proc SPIE 4259
7. Draxler S, Lippitsch ME (1996) Lifetime-based sensing: influence of the microenvironment. Anal Chem 68:753–757
8. Malins C, Glever HG, Keyes TE, Vos JG, Dressick WJ, MacCraith BD (2000) Sol-gel immobilized ruthenium(II) polypyridyl complexes as chemical transducers for optical pH sensing. Sensors Actuators B Chem 67:89–95
9. Price JM, Xu W, Demas JN, Degraff BA (1998) Polymer-supported pH sensor based on Hydrophobically bound Luminecent ruthenium(II) complexes. Anal Chem 70:265–270
10. Carmody WR (1961) Easily prepared wide range buffer series. J Chem Educ 38:559
11. Ryder AG, Power S, Glynn TJ (2003) Evaluation of Acridine in Nafion as a fluorescence-lifetime-based pH sensor. Appl Spectrosc 57:73–79
12. Ryder AG, Power S, Glynn TJ (2003) Fluorescence-lifetime-based pH sensing using Resorufin. SPIE, OPTO Ireland
13. van der Maaden K, Sliedregt K, Kros A, Jiskoot W, Bouwstra J (2012) Fluorescent nanoparticle adhesion assay: a novel method for surface pKa determination of self-assembled monolayers on silicon surfaces. Langmuir 28:3403–3411
14. Vezenov DV, Noy A, Rozsnyai LF, Lieber CM (1997) Force titrations and ionization state sensitive imaging of functional groups in aqueous solutions by chemical force microscopy. J Am Chem Soc 119:2006–2015
15. Mengistu TZ, Goel V, Horton JH, Morin S (2006) Chemical force titrations of functionalized Si(111) surfaces. Langmuir 22:5301–5307
16. Diverdi LA, Topp MR (1984) Subnanosecond time-resolved fluorescence of Acridine in solution. J Phys Chem 88:3447–3451

17. Dong Y, Pappu SV, Xu Z (1998) Detection of local density distribution of isolated Silanol groups on planar silica surfaces using nonlinear optical molecular probes. Anal Chem 70:4730–4735
18. Ong S, Zhao X, Eisenthal KB (1992) Polarization of water molecules at a charged Interface: second harmonic studies of the silica/water Interface. Chem Phys Lett 191:327–335
19. Bakker HJ, Physical Chemistry (2012) Water's response to the fear of water. Nature 491:533–535
20. Nilsson A, Pettersson LGM (2015) The structural origin of anomalous properties of liquid water. Nature Comm 6:8998
21. Lowe BM, Skylaris C-K, Green NG (2015) Acid-Base dissociation mechanisms and energetics at the silica–water Interface: an Activationless process. J Colloid Interface Sci 451:231–244
22. Wolfbeis OS, Urbano E (1983) Fluorescence quenching method for determination of two or three components in solution. Anal Chem 55:1904–1906
23. Draxler S, Lippitsch ME (1995) pH sensors using fluorescence decay time. Sensors Actuators B Chem 29:199–203